Analecta Technica Szegedinensia

Vol. 18, No. 3 ISSN 2064-7964 2024

MECHANICAL PROPERTIES AND MICROSTRUCTURAL CHARACTERISTICS OF STEEL PIPES AFTER LONG-TIME HYDROGEN EXPOSURE

[1]Nóra Nagy, [1]János Lukács

[1]University of Miskolc, Egyetemváros, 3515, Miskolc, Hungary,

[1]e-mail: nora.nagy@uni-miskolc.hu, [2]e-mail: janos.lukacs@uni-miskolc.hu

Received: 3rd June	*Accepted: 19th September*

ABSTRACT

There are three possibilities to transport hydrogen by high pressure pipeline (i) blending hydrogen into the existing natural gas pipeline system, (ii) after checking the integrity, using the natural gas transporting pipeline system to transport hydrogen, (iii) building a new pipeline system to transport pure hydrogen. In all three cases should be known the behaviour of the pipe material and its welded joints influenced under high pressure hydrogen. For this aim pipeline sections made of P355NH base material were investigated without and with hydrogen exposure, where the exposure time was 41 days. Gas metal arc welding and hybrid tungsten arc welding / gas metal arc welding were applied for preparation of the girth weld joints. Tensile, three point bending and hardness tests, furthermore microstructural investigations were performed both on base materials and girth welds of the pipeline sections. The testing results were analysed and compared with each other (base material vs. welded joints, without exposure vs. with exposure) and with limit values can be found in the literature. Conclusions were drawn on the behaviour of the investigated pipe material and its welded joints.

Keywords: transporting pipeline, hydrogen, welding, mechanical behaviour, microstructural characteristics

1. INTRODUCTION

Hydrogen embrittlement (HE) results in a reduction in the fracture toughness or ductility of the material due to the presence of atomic hydrogen. Fracture usually occurs at stress levels below the yield strength of the material. Hydrogen embrittlement through hydrogen-metal interaction can be divided into three categories: hydrogen environmental embrittlement (HEE), internal hydrogen embrittlement (IHE) and hydrogen reaction embrittlement (HRE). In general, HEE refers to the condition where materials are exposed to a high-pressure gaseous hydrogen environment. The definition of IHE suggests that the source of hydrogen is usually not from a high-pressure gaseous system, but from hydrogen electrochemical processes. The definition of HRE is generally irreversible hydrogen damage due to chemical reaction with hydrogen, which can occur without external stress (Figure 1) [1].

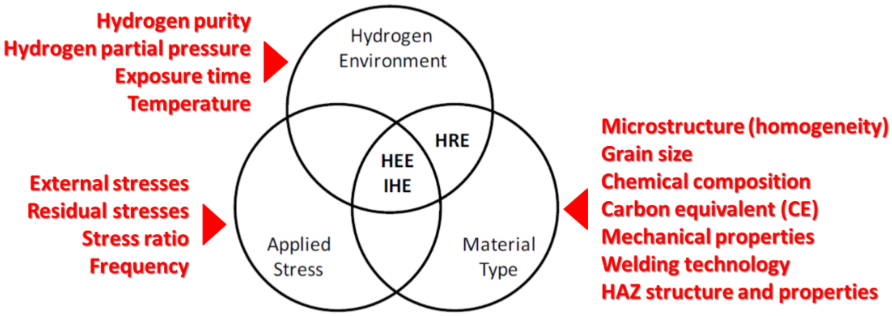

Figure 1. Classification of HEE, IHE and HRE type based hydrogen, stress, and material factors [1]

Among the susceptibility factors, material side was investigated in our research, taking into account microstructural factors for both the base material and welded joints. Microstructure plays a key role in

DOI: https://doi.org/10.14232/analecta.2024.3.28-38

hydrogen adsorption and diffusion. The different details of the microstructure are called hydrogen traps, which can be reversible or irreversible depending on the strength of the interaction with hydrogen. From a thermodynamic point of view, traps represent a lower chemical potential for hydrogen and require a higher activation energy to pass through them [2]. The crystal structure, the number and size of interstitial sites and the orientation of the crystalline planes influence the hydrogen trapping efficiency [3]. Dislocations are reversible hydrogen traps due to their low binding energy [4]. The interaction between hydrogen and dislocations can be explained by the Cottrell atmosphere around the dislocations [5]. Ref. [6] found that diffusion generally decreases with increasing dislocation density. In general, with respect to grain structure, the type, size and distribution of grains determine the hydrogen adsorption [7-8]. Hydrogen atoms can agglomerate between the different phases of the grains or at the grain boundaries, hindering further diffusion of hydrogen, but they are not considered irreversible traps [9]. Grain boundaries are also reversible hydrogen traps through which hydrogen diffuses under the influence of lower energies and studies show that the diffusion rate of hydrogen increases in fine-grained microstructures, but the opposite effects have been observed for trinuclear junctions, which can act as potential hydrogen traps and reduce the diffusion of hydrogen [10].

2. INVESTIGATED STEEL PIPES

The investigated pipeline sections were made of P355NH material which is one of the common material grades used for domestic transmission pipelines. Fatigue and burst tests were carried out on the investigated pipeline sections [11], therefore before the hydrogen exposure, these pipeline sections were redesigned and rebuilt as shown in Figure 2. The original pipeline sections were made of P355NH seamless steel pipes [12] with nominal diameter DN 100 and nominal wall thickness of 5.6 mm. The nominal length of the originally tested sections was 4,000 mm. The nominal length of the redesigned and rebuilt sections was only 1,100 mm.

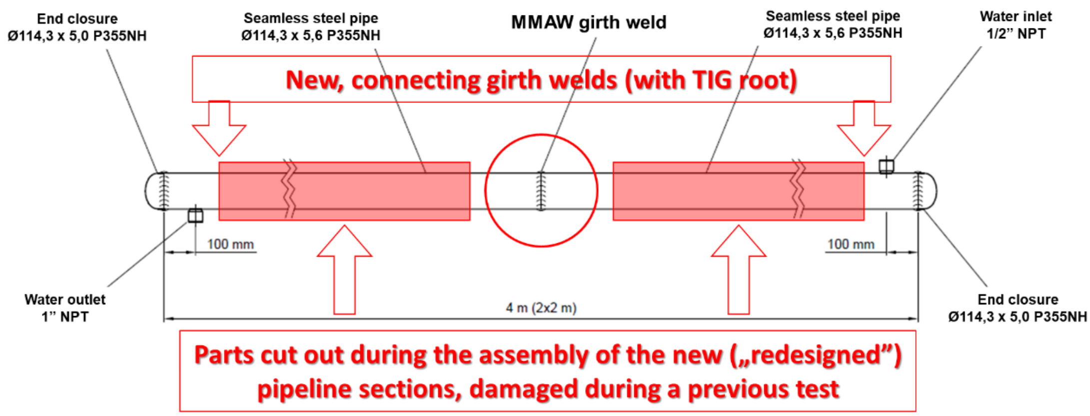

Figure 2. The original (Y3, black) and the redesign pipeline-section (HY4, red)

The hydrogen exposure was executed at the Linde Gas Hungary Ltd. site in Budapest, at twice the Maximum Allowable Operating Pressure (128 bar) in pure hydrogen. To analyse the effects of 41 days of hydrogen exposure, tensile, bending and hardness tests, as well as microstructural investigations were carried out on both the materials and the girth welds of the pipeline sections.

DOI: https://doi.org/10.14232/analecta.2024.3.28-38

Analecta Technica Szegedinensia
Vol. 18, No. 3 ISSN 2064-7964 2024

2.1. Base material and the welded joints

The microstructure of the P355NH test material is ferrite-pearlite, with a ferrite-pearlite ratio of approximately 80%-20%. Microscopic images were taken with a Zeiss Axio Observer Dm1 inverted optical microscope (Figure 3).

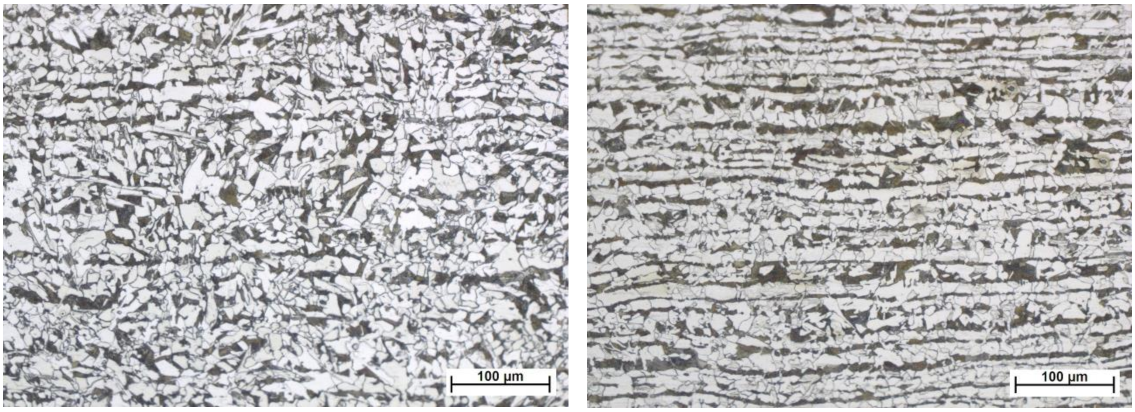

Figure 3. The base material without (Y3) and with (HY4) hydrogen exposure, N=200x, etched: 2% HNO_3

The tested girth welds (Figure 4) were made using manual metal arc welding, while the new, connecting (non-testing) girth welds (hybrid welds) were fabricated under workshop conditions, applying TIG welding (root) and metal arc welding (further layers). The hybrid welded joint was not tested without hydrogen, so results are only reported where a comparison with the other weld was meaningful in some respect.

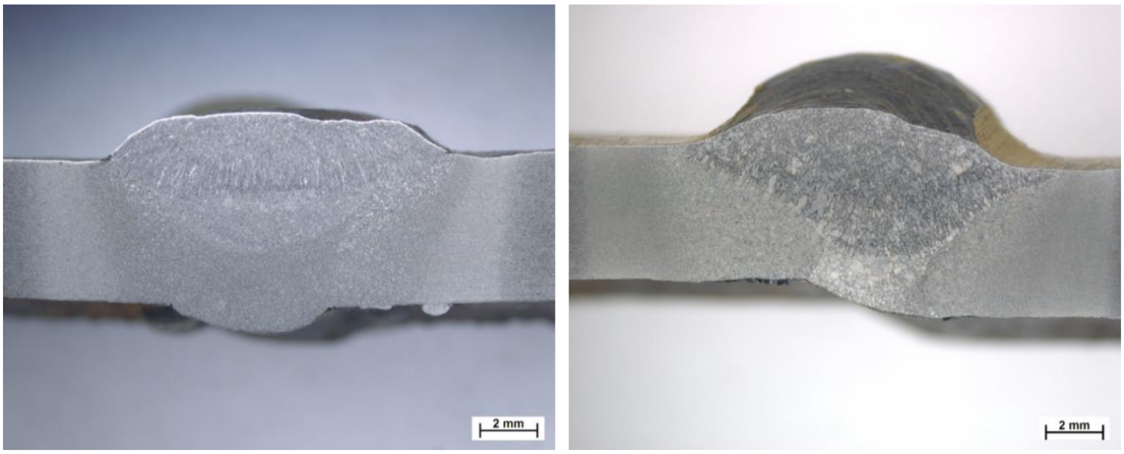

a) MMAW *b) hybrid*

Figure 4. Macro images of the welded joints, N=6,5x

3. THREE-POINT BENDING TEST

The three-point bending test is one of the simplest methods for assessing the embrittlement of materials. The test involves placing the specimens on two support rollers and bending them to an angle of 180°. No cracking was observed in either the base material or the welded joints up to the specified bending angle. Some typical images of the blending surfaces are shown in Figure 5.

DOI: https://doi.org/10.14232/analecta.2024.3.28-38

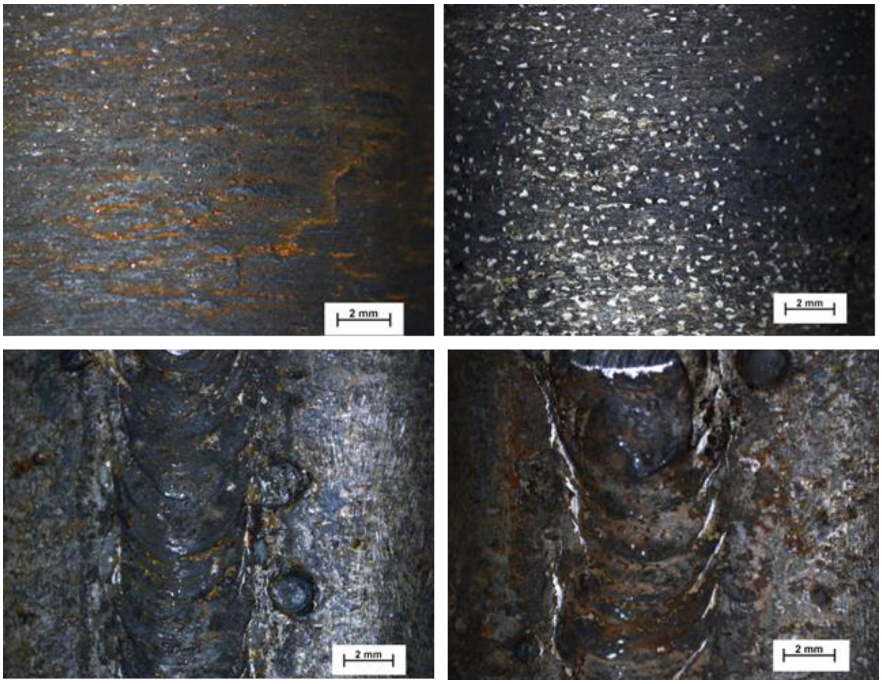

a) without hydrogen *b) with 41-days hydrogen exposure*

Figure 5. Macro images of the bending surfaces of the base material (on the top) and of the welded joint (bottom), N=6,5x

4. TENSILE TESTS

To assess the embrittlement of steels exposed to hydrogen in tensile testing, strain properties and their ratios are primarily used because they are a better expression of the susceptibility to potential embrittlement than strength indices. These include the percentage elongation at break (A) or elongation ratio (A_{ratio}), the reduction of area (Z) or contraction ratio (Z_{ratio}) and the embrittlement index (EI), which can be calculated using equation, as follows:

$$A_{ratio} = \frac{A_{hydrogen\ environment}}{A_{air}}, \tag{1}$$

$$Z_{ratio} = \frac{Z_{hydrogen\ environment}}{Z_{air}}, \tag{2}$$

$$EI = \frac{(Z_{air} - Z_{hydrogen})}{Z_{air}}. \tag{3}$$

The hydrogen embrittlement categories are summarized in Table 1 based on the literature [13].

Table 1. Hydrogen embrittlement categories [13]

Categories	Embrittlement Index (EI)
negligible	0.00 - 0.03
small	0.04 – 0.10
high	0.11 – 0.30
severe	0.31 – 0.50
extreme	0.51 – 1.00

DOI: https://doi.org/10.14232/analecta.2024.3.28-38

The tests were carried out on a MTS 810.23 universal materials testing machine. The elongation of the flat specimens was measured with an extensometer. The measured values of the previously presented metrics for the tested steel and welded joints are shown in Figures 6-8.

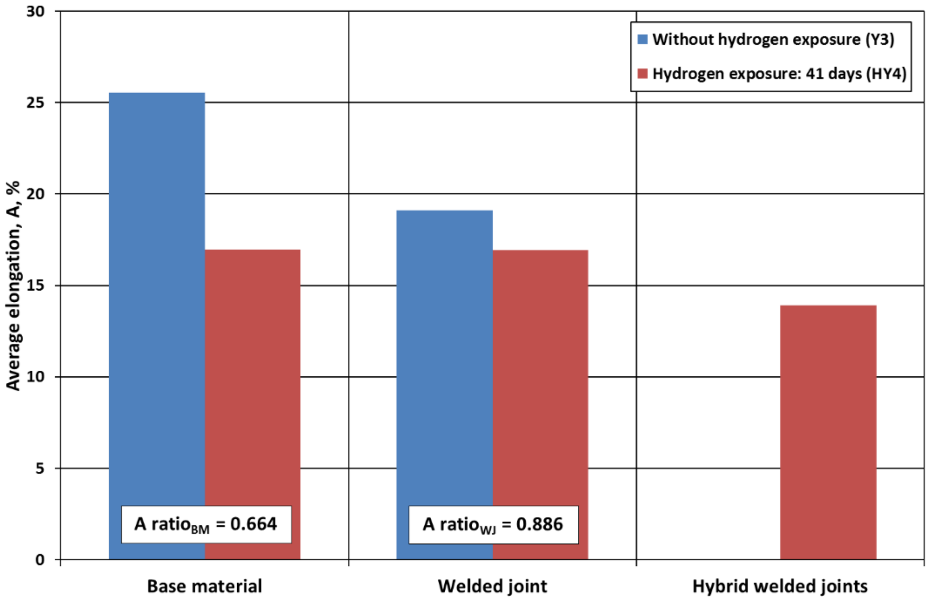

Figure 6. Influence of hydrogen exposure on the average of the elongation and the A_{ratio} values

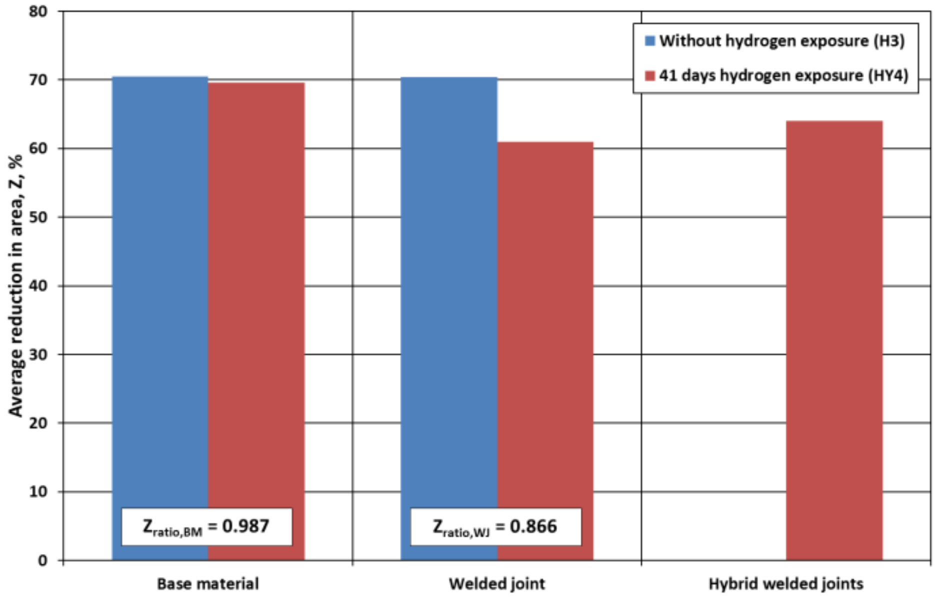

Figure 7. Influence of hydrogen exposure on the average of the reduction of area and the Z_{ratio} values

DOI: https://doi.org/10.14232/analecta.2024.3.28-38

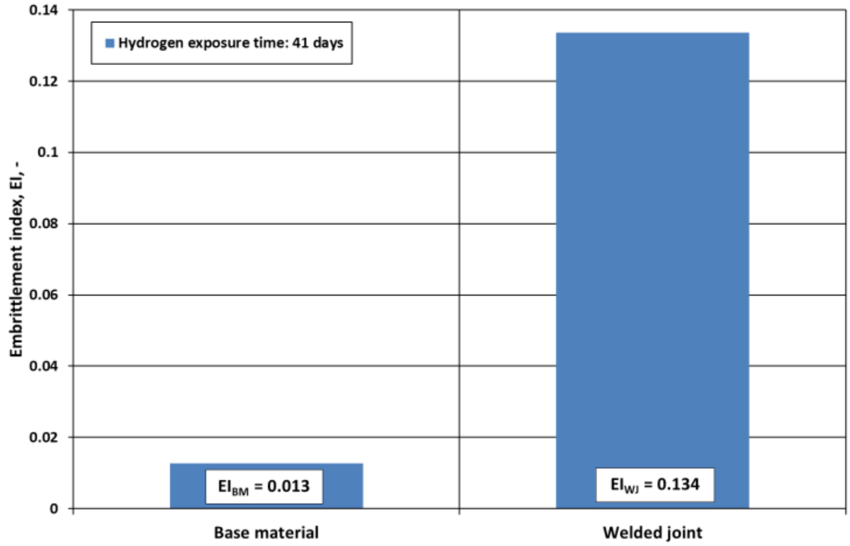

Figure 8. Embrittlement index values after 41 days of hydrogen exposure

5. HARDNESS MEASUREMENTS

For the hardness measurements, samples of both the base material and welded joints were taken from both the non-hydrogen and hydrogen-exposured pipeline-sections near the root side. Hardnesses were measured using a Wilson-Hardness Reicherter UH-250. HV5 hardness values were determined, in accordance with microscopic images, to isolate the heat affected zones of the welded joints (Figure 9). In the diagrams (Figure 10), samples marked with an H indicate the exposure to hydrogen. For welded joints, V indicates a MMAW joint and W indicates a TIG root joint. As can be seen in Figure 9, the hardness of the base material increased due to hydrogen exposure.

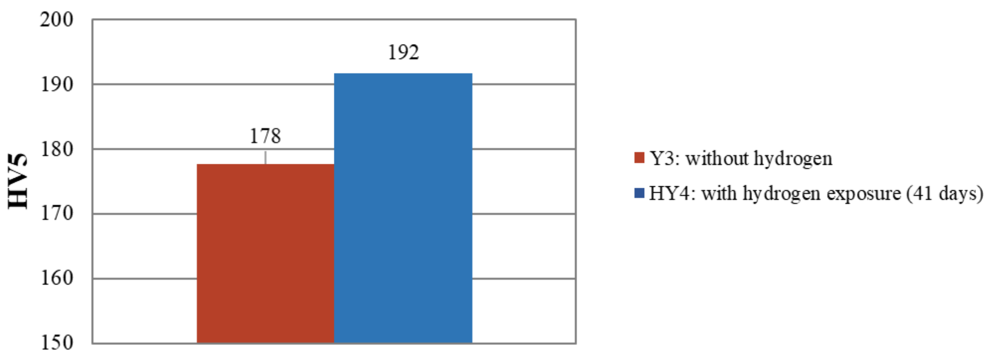

Figure 9. Average HV5 hardness values of the base materials

Figure 10 shows the hardness distributions of the welded joints. Both technologies show the usual trends. In the case of MMAW, the increase in hardness is clearly visible.

DOI: https://doi.org/10.14232/analecta.2024.3.28-38

Analecta Technica Szegedinensia
Vol. 18, No. 3 ISSN 2064-7964 2024

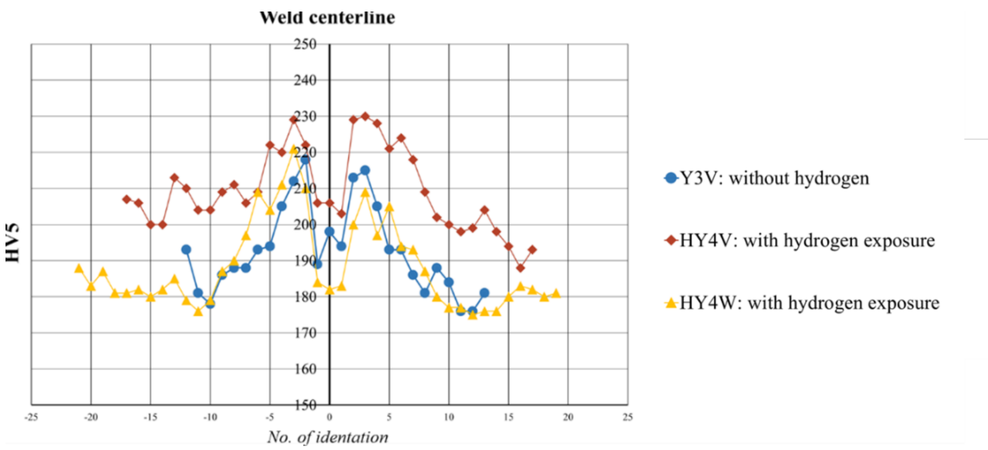

Figure 10. Hardness distributions on the root side of the investigated girth welds

When looking at the heat affected zones, the increase was larger in the intercritical zone of HY4V joint. The HY4W joint showed no change. Microscope images (Figure 12) show that in the intercritical zone of the heat affected zones, the ferrite is slightly finer grained for HY4W than for HY4V.

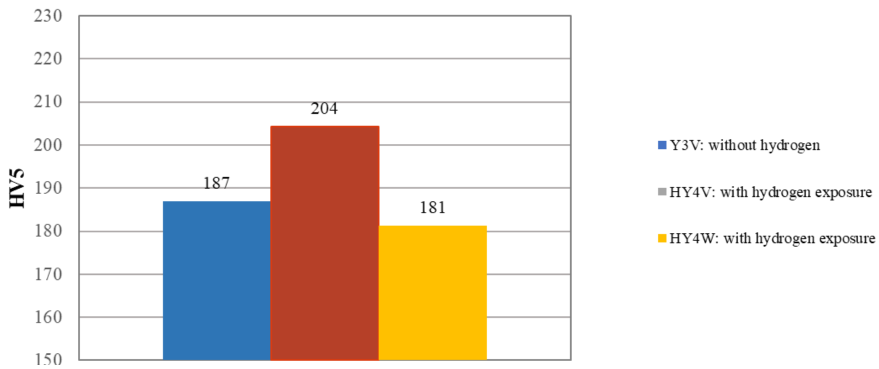

Figure 11. Results of hardness measurements in the intercritical zone

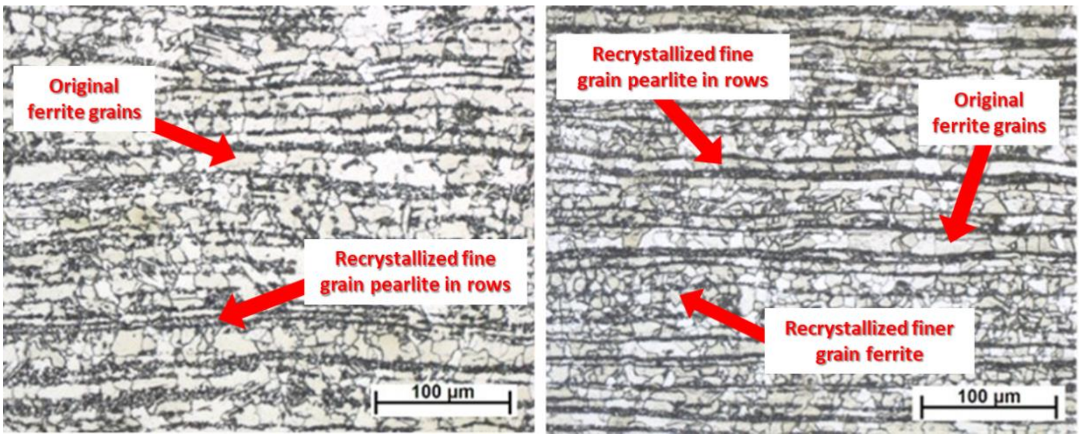

a) HY4V ***b) HY4W***

Figure 12. Intercritical zones of the heat affected zone of welded joints, N=200x, etched: 2% HNO_3

DOI: https://doi.org/10.14232/analecta.2024.3.28-38

For the recrystallized zone (Figure 13), a significant increase in hardness is observed in the joints made by the MMAW process. The hardness of the joints made with the TIG root did not change significantly here either. A typical record of the recrystallized zone for joints prepared by different processes is shown in Figure 14.

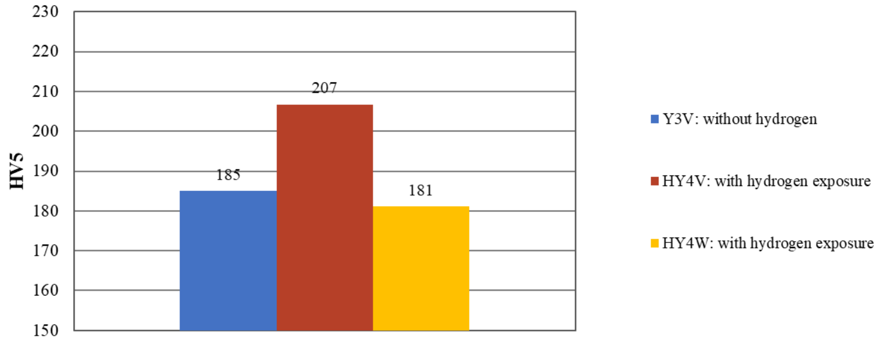

Figure 13. Results of hardness measurements in the recrystallized zone

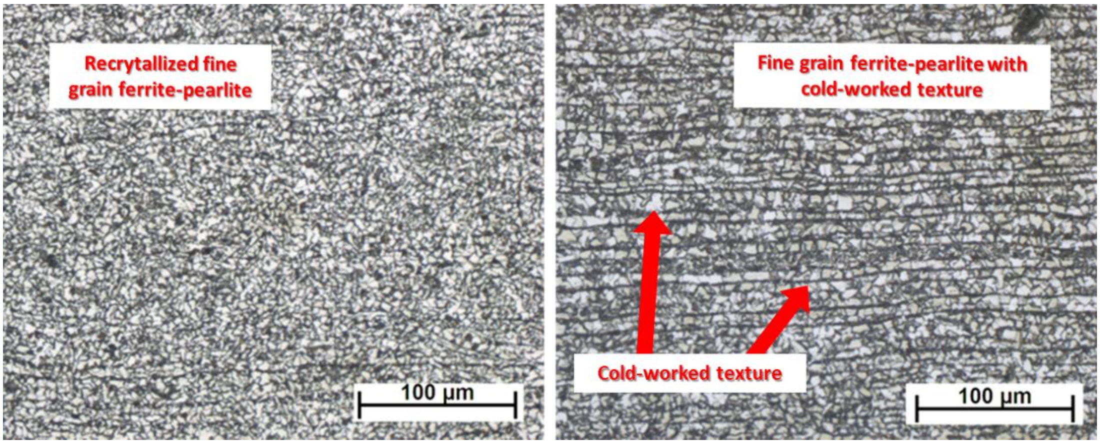

a) HY4V ***b) HY4W***

Figure 14. Recrystallized zones of the heat affected zone of welded joints, N=200x, etched: 2% HNO_3

In the coarse grained zones of the joints (Figure 15), there is a significant increase in hardness for both MMAW and TIG/MMAW hybrid joints.

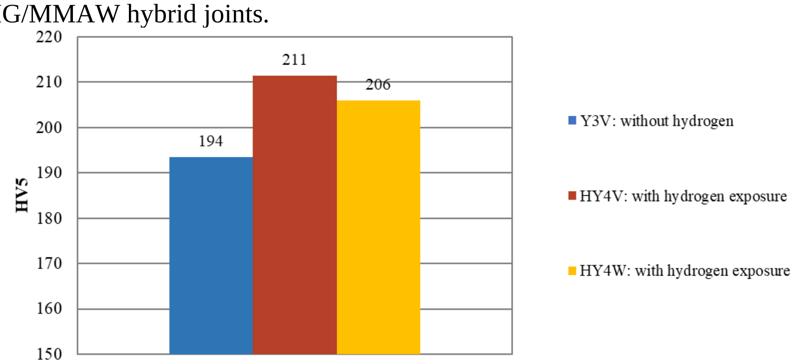

Figure 15. Results of hardness measurements in the coarse grained zone

DOI: https://doi.org/10.14232/analecta.2024.3.28-38

Analecta Technica Szegedinensia
Vol. 18, No. 3 ISSN 2064-7964 2024

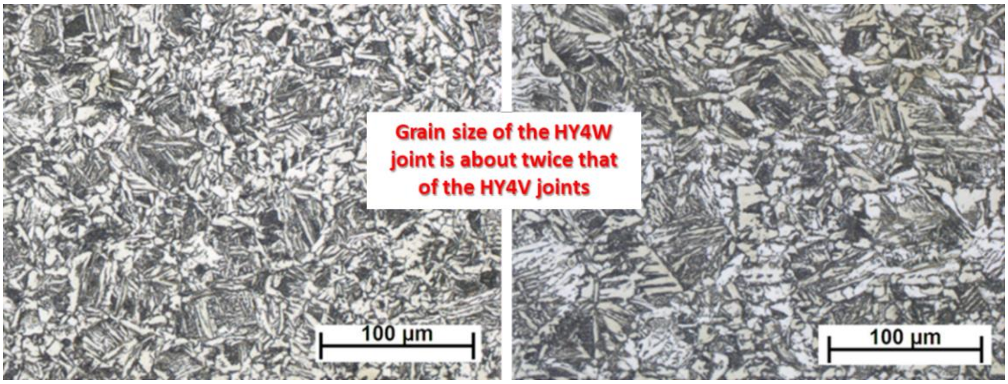

a) HY4V *b) HY4W*

Figure 16. Coarse grained zones of the heat affected zone of welded joints, N=200x, etched: 2% HNO_3

Based on the hardness values measured on the weld roots (Figure 17), it can be concluded that the MMAW joints showed a smaller increase in hardness. The hardness of the TIG root did not change significantly. The microstructure of the weld roots shown in Figure 18 has different proportions of bainitic and tempered martensitic parts. It can be clearly seen that the amount of tempered martensite in the TIG joint is obviously higher than in the MMAW joint.

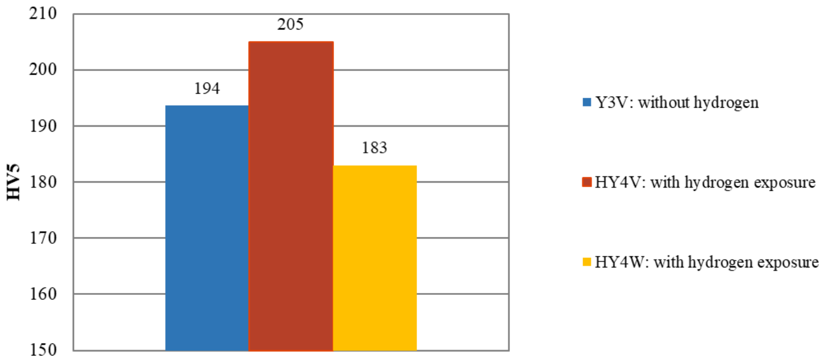

Figure 17. Results of the hardness measurement in the weld root

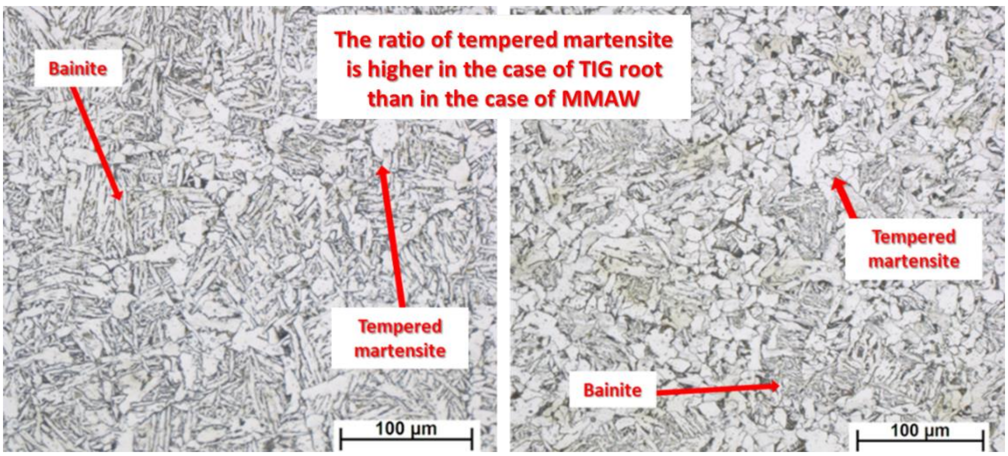

a) MMAW root *b) TIG root*

Figure 18. Roots of the welded joints, N=200x, etched: 2% HNO_3

DOI: https://doi.org/10.14232/analecta.2024.3.28-38

6. CONCLUSIONS

Based on the investigations carried out and a combined evaluation of the test results, the following conclusions can be drawn.

I. Based on the results of the bending tests carried out, no macroscopic embrittlement was observed in either the base material or the welded joints.
II. The hardness distributions measured on the welded joints correspond to the hardness distributions expected for the welding technologies used. The increase in hardness measured after 41 days of hydrogenation is considered significant for the MMAW joint.
III. The elongation at break and reduction of area in the tensile test specimens, as well as the embrittlement index resulting from the percent reduction of area values, indicate the adverse effect of hydrogen exposure. There are not yet sufficient data to confirm whether the adverse effects differ significantly between the parent and welded joints or between hybrid welded joints.
IV. In the case of hardness measurements, higher hardness values for MMAW joint after exposure to hydrogen than for TIG joints were typically measured.
V. For the MMAW joints, the hardness was higher in the coarse grained and recrystallized heat affected zones after hydrogen exposure. In the case of TIG joints, the increase was measured in the coarse grained zone critical for the steel tested. The criticality for the steel tested thus makes it likely that these microstructural regions are more susceptible to hydrogen embrittlement for the test joints.
VI. Based on the hardness tests, the joints of the P355NH steel tested with the TIG technology are less sensitive and therefore the risk of hydrogen embrittlement is expected to be lower for this type of joint.

REFERENCES

[1] Lee J.A. Hydrogen Embrittlement NASA/TM—2016–218602, *NASA* Marshall Space Flight Center Huntsville, Alabama, April 2016; 50p. Available online: https://ntrs.nasa.gov/api/citations/20160005654/downloads/20160005654.pdf
[2] Oriani, R. (1970). The diffusion and trapping of hydrogen in steel. *Acta Metallurgica*, 18(1), 147–157. https://doi.org/10.1016/0001-6160(70)90078-7.
[3] Brass, A.-M., Chene, J., & Coudreuse, L. (2000). Fragilisation des aciers par l'hydrogène mécanismes. *Corrosion Vieillissement*. https://doi.org/10.51257/a-v2-m176
[4] Choo, W. Y., & Jai Young Lee. (1983). Effect of cold working on the hydrogen trapping phenomena in pure iron. *Metallurgical Transactions*. A, Physical Metallurgy and Materials Science, 14(7), 1299–1305. https://doi.org/10.1007/bf02664812
[5] Cotterill, P. (1961). The hydrogen embrittlement of metals. Progress in Materials Science, 9(4), 205–301. https://doi.org/10.1016/0079-6425(61)90005-6
[6] Cabrini, M., Coppola, L., Lorenzi, S., Testa, C., Carugo, F., Bucella, D. P., & Pastore, T. (2020). Hydrogen Permeation in X65 Steel under Cyclic Loading. Materials, 13(10), 2309. https://doi.org/10.3390/ma13102309
[7] Anijdan, S. M., Arab, G., Sabzi, M., Sadeghi, M., Eivani, A., & Jafarian, H. (2021). Sensitivity to hydrogen induced cracking, and corrosion performance of an API X65 pipeline steel in H2S containing environment: influence of heat treatment and its subsequent microstructural changes. *Journal of Materials Research and Technology/Journal of Materials Research and Technology*, 15, 1–16. https://doi.org/10.1016/j.jmrt.2021.07.118
[8] Park, G. T., Koh, S. U., Jung, H. G., & Kim, K. Y. (2008). Effect of microstructure on the hydrogen trapping efficiency and hydrogen induced cracking of linepipe steel. *Corrosion Science*, 50(7), 1865–1871. https://doi.org/10.1016/j.corsci.2008.03.007
[9] Tau, L., & Chan, S. L. I. (1996). Effects of ferrite/pearlite alignment on the hydrogen permeation in a AISI 4130 steel. *Materials Letters*, 29(1-3), 143–147. https://doi.org/10.1016/s0167-577x(96)00140-1

DOI: https://doi.org/10.14232/analecta.2024.3.28-38

[10] Ichimura, M., Sasajima, Y., & Imabayashi, M. (1991). Grain boundary effect on diffusion of hydrogen in pure aluminum. *Materials Transactions,* 32(12), 1109–1114. https://doi.org/10.2320/matertrans1989.32.1109

[11] Lukács, J., & Dakhel, A. Y. (2024). Full-scale Fatigue and Burst Tests on Notched Pipeline Girth Welds, under Complex Loading Conditions. *Acta Polytechnica Hungarica*, 21(5), 53–70. https://doi.org/10.12700/aph.21.5.2024.5.5

[12] EN 10216-3: Seamless steel tubes for pressure purposes. Technical delivery conditions Alloy fine grain steel tubes. Brussels: European Committee for Standardization, 2013.

[13] Campari A, Ustolin F, Alvaro A, et al. (2023) A review on hydrogen embrittlement and risk-based inspection of hydrogen technologies. *International Journal of Hydrogen Energy*, 48(90):35316-35346.